

Enhancement of Phototransduction Protein Interactions by Lipid Surfaces*

(Received for publication, August 19, 1999, and in revised form, October 28, 1999)

Thomas J. Melia‡, Justine A. Malinski§, Feng He, and Theodore G. Wensel¶

From the Verna and Marrs McLean Department of Biochemistry, Baylor College of Medicine, Houston, Texas 77030

The G protein cascade of vision depends on two peripheral membrane proteins: the G protein, transducin (G_t), and cGMP phosphodiesterase (PDE). Each has covalently attached lipids, and interacts with transduction components on the membrane surface. We have found that their surface interactions are critically dependent on the nature of the lipid. Membranes enhance their protein-protein interactions, especially if electrostatic attraction is introduced with positively charged lipids. These interactions are less enhanced on highly curved surfaces, but are most enhanced by unsaturated or bulky acyl chains. On positively charged membranes, G_t assembles at a high enough density to form two-dimensional arrays with short-range crystalline order. Cationic membranes also support extremely efficient activation of PDE by the GTP γ S (guanosine 5'-O-(thiotriphosphate)) form of G_{α_t} (G_{α_t} -GTP γ S), minimizing functional heterogeneity of transducin and allowing activation with nanomolar G_{α_t} -GTP γ S. Quantification of PDE activation and of the amount of G_{α_t} -GTP γ S bound to PDE indicated that G_t activates PDE maximally when bound in a 1:1 molar ratio. No cooperativity was observed, even at nanomolar concentrations. Thus, under these conditions, the one binding site for G_{α_t} -GTP γ S on PDE that stimulates catalysis must be of higher affinity than one or more additional sites which are silent with respect to activation of PDE.

Transduction of extracellular signals into intracellular responses by heterotrimeric G proteins (reviewed in Ref. 1) is dominated by protein-protein interactions occurring on the cytoplasmic surfaces of membranes containing heptahelical receptors. G protein subunits convey information between transmembrane receptors and effectors that are also typically either integral or peripheral membrane proteins. Regulators of transduction, such as receptor kinases, arrestin, and its homologues, and GTPase accelerating proteins, are also often localized to the signaling domains of cell membranes. Localization of multiple cascade components may be important for achieving specificity of interactions, and rapid tightly coupled responses.

The G protein cascade of vision has served as a useful model system for studying the role of lipid membranes in signal

transduction. Both the G protein transducin (G_t)¹ and its effector, cGMP phosphodiesterase (PDE) are normally associated with the surface of disc membranes in rod outer segments, and each contains two covalently attached lipids: farnesyl and geranylgeranyl groups on PDE α and PDE β , respectively (2), and NH₂-terminal fatty acid (3–6) and COOH-terminal farnesyl (7, 8) on G_{α_t} and G_{γ_t} , respectively. However, these lipids confer only modest membrane affinity, and both PDE and G_t can be selectively extracted without use of detergents, and purified by chromatography. Interactions between activated forms of the α subunit of the G protein, *e.g.* G_{α_t} -GTP γ S, and PDE can be reconstituted using the purified proteins, and show a strong membrane dependence (9–13).

The utility of these reconstitution experiments has been limited by the relatively low efficiency of PDE activation observed in them, as compared with that inferred from the physiology of intact cells where activation occurs on a millisecond time scale with low levels of activated G_t . Reconstitution experiments have typically required micromolar levels of G_{α_t} -GTP γ S, even with nanomolar PDE (12, and references cited therein). Detailed analysis of the dependence of PDE activity on added G_{α_t} -GTP γ S has suggested that functional heterogeneity of G_t is likely responsible for the low reconstitution efficiency. Conformational heterogeneity involving the membrane-binding domains of G_t seems a likely candidate for this phenomenon, because membrane binding and activation are strongly correlated (12, 14). A practical consequence of this G_t heterogeneity and inefficient activation has been difficulty in determining the stoichiometric ratio of subunits in the PDE- G_{α_t} -GTP γ S complex. PDE contains two homologous catalytic subunits, PDE α and PDE β , as well as two inhibitory PDE γ subunits (15), each of which can bind tightly ($K_d < 1$ nM) to G_{α_t} -GTP γ S (16). It has been widely assumed that there are two binding sites for G_{α_t} -GTP γ S on PDE, and some experimental evidence (*e.g.* Ref. 11) supports this idea, but the high concentrations needed to observe full occupation of these sites has obstructed accurate correlation of PDE activity with site occupation. Indeed, three mutually exclusive models have been proposed: 1) two sites of approximately equal affinity and equal contributions to catalytic activity (17); 2) one higher affinity site contributing 80–100% of the catalytic activity, with a second, lower affinity site contributing much less (13); and 3) a higher affinity site contributing 30% or less of the catalytic activity, with occupation of a second lower affinity site needed for full activation (18, 19). In addition, cooperativity between

* The costs of publication of this article were defrayed in part by the payment of page charges. This article must therefore be hereby marked "advertisement" in accordance with 18 U.S.C. Section 1734 solely to indicate this fact.

‡ Current address: Cellular Biochemistry and Biophysics Program, Memorial Sloan-Kettering Cancer Center, 1275 York Ave., New York, NY 10021.

§ Current address: ATG Laboratories, Inc., 10300 Valley View Rd., Eden Prairie, MN 55344.

¶ To whom correspondence should be addressed: Dept. of Biochemistry, Baylor College of Medicine, One Baylor Plaza, Houston, TX, 77030. Tel.: 713-798-6994; Fax: 713-796-9438; E-mail: twensel@bcm.tmc.edu.

¹ The abbreviations used are: G_t , transducin G protein; PDE, cGMP phosphodiesterase (PDE6); DOPC, dioleoylphosphatidylcholine; DOTAP, dioleoyltrimethylammonium propane; DSTAP, distearoyltrimethylammonium propane; PC, egg phosphatidylcholine; PS, phosphatidylserine; PE, phosphatidylethanolamine; MOPS, 4-morpholinopropanesulfonic acid; SUV, small unilamellar vesicle; LUV, large unilamellar vesicle; sl-LUV, sucrose-loaded large unilamellar vesicle; ROS, rod outer segments; GTP γ S, guanosine 5'-O-(thiotriphosphate).

the two sites has been proposed (20), and functional differences between the two PDE γ sites in trypsinized PDE have been identified through differential interactions with mutant PDE γ (21).

In order to understand better the role of membrane lipids in G $_t$ signaling, we have reconstituted on synthetic lipid vesicles two different G $_{\alpha\beta\gamma}$ -containing complexes: G $\alpha\beta\gamma$ -GDP, and PDE-G α_t -GTP γ S, and explored the role of vesicle properties in the binding and activity of these complexes. This work was undertaken to answer three key questions: 1) how does lipid composition affect binding of G $_t$ to membranes and membrane-dependent activation of PDE by G α_t -GTP γ S? 2) Can a lipid surface be found that enhances binding of G $_t$ and the G α_t -GTP γ S-PDE complexes sufficiently for structural analysis by electron crystallography? 3) If PDE activation by G $_t$ is sufficiently enhanced to allow most G α_t -GTP γ S to participate in PDE activation, what is the relationship between PDE activity and number of G α_t -GTP γ S molecules bound?

MATERIALS AND METHODS

Reagents—Frozen dark-adapted bovine retinas were purchased from J. A. Lawson Packing (Lincoln, NE). Rhodamine-dipalmitoylphosphatidylethanolamine was obtained from Molecular Probes, stearylamine from Sigma, and all other lipids were from Avanti Polar Lipids Inc.

Buffers—PDE assay buffer: 10 mM MOPS, 1 mM MgCl $_2$, 0.1 mM EDTA, pH 8.0, with NaCl or KCl added to the indicated concentrations. The ROS buffer was: 10 mM MOPS, 1 mM MgCl $_2$, 30 mM NaCl, 60 mM KCl, 1 mM dithiothreitol, pH 7.4. Low salt 1 buffer consisted of: 5 mM Tris, 0.5 mM MgCl $_2$, 1 mM dithiothreitol, pH 7.4. The Low salt 2 buffer was: 10 mM MOPS, 2 mM MgCl $_2$, 1 mM dithiothreitol, pH 7.4. Low salt 3: 20 mM MOPS, 2 mM MgCl $_2$, 0.2 mM EDTA, pH 8.0. DEAE load buffer was: 10 mM MOPS, 10 mM MgCl $_2$, 1 mM dithiothreitol, pH 8.0. All buffers were filtered through 0.2- μ m pore nitrocellulose.

ROS Membrane and Protein Purification—Rod outer segment membranes (ROS) were isolated from frozen bovine retina on sucrose gradients under dim red light according to established methods (22). Urea-washed membranes which have had peripheral membrane proteins removed, were prepared by a series of washing steps, including 4 M urea as described previously (23).

G $_t$ and G α_t -GTP γ S were purified essentially as described (12, 24, 25). Briefly, ROS membranes (15–25 μ M) were bleached and washed in ROS buffer followed by multiple washes in Low salt 1 buffer. G $_t$ was extracted from the membranes in Low salt 1 buffer + GTP, loaded onto a hexyl-agarose column (Sigma) and purified by step elution with Low salt 2 buffer + NaCl. Hexyl-agarose-purified G $_t$ was ~95% pure by Coomassie staining on SDS-polyacrylamide gel electrophoresis gels. For G α_t -GTP γ S, either G $_t$ was extracted from ROS with Low salt 1 + GTP γ S, or hexyl-agarose-purified G $_t$ was activated with a catalytic amount of urea-washed ROS in the presence of GTP γ S and a trace amount of GTP- γ - 35 S. G α_t -GTP γ S was separated from G $\beta\gamma$ by loading onto a Reactive Blue 2-Sepharose CL-6B column (Sigma) and eluted in increasing [KCl]. In some cases, G $_t$ or G α_t -GTP γ S were further purified by high performance liquid chromatography anion-exchange, as described (12).

PDE was purified from Low salt 1 extracts of ROS by loading onto a hydroxylapatite column in 30 mM phosphate and 50 mM NaCl (Bio-Rad HTP dry hydroxylapatite (12)), followed by step elution in increasing phosphate. In most cases (Figs. 4–7), PDE was further purified by concentrating PDE-containing fractions and exchanging into DEAE load buffer immediately before loading onto a high performance liquid chromatography anion-exchange column. (Waters DEAE-5PW). PDE was eluted with increasing [NaCl]; data in Fig. 3 are from PDE not subjected to this second chromatography step. Purified proteins were concentrated with a Centricon-30 and stored at –20 °C in 40–50% (v/v) glycerol. Recombinant PDE γ was expressed in *Escherichia coli* as a fusion protein and purified as described (26).

Proteolysis—To measure maximal, trypsin-generated PDE activity, PDE was treated with trypsin (0.05–0.1 mg/ml final) in pH assay buffer at the indicated [NaCl] or [KCl], while activity was monitored continuously as described below. For experiments testing PDE-membrane interactions with and without PDE's lipid modified membrane-binding domains, PDE was treated with trypsin in PDE assay buffer (50 mM NaCl) at PDE:trypsin = 100:1 for 8 min at room temperature and then soybean trypsin inhibitor was added at a 10-fold excess over trypsin to stop the reaction. Recombinant PDE γ was added back at a slight excess

over the amount required to inhibit trypsinized PDE activity.

G α_t was proteolyzed to remove the fatty acylated NH $_2$ terminus involved in membrane binding (27). G α_t -GTP γ S (12.5 μ M) was incubated with 333 nM endoproteinase Lys-C (Sigma) for 30 min at room temperature and then the reaction was stopped by addition of the proteinase inhibitors, aprotinin and leupeptin (22-fold excess mol/mol). The efficiency of proteolysis was determined using a monoclonal antibody (mAb4A) which recognizes only the myristoylated NH $_2$ terminus of G $_t$ (27).² A 30-min incubation was sufficient to remove all mAb4A-binding sites; the reaction was 80–90% complete within 5 min.

Protein Determination—Concentrations of PDE, G $_t$, and G α_t -GTP γ S were routinely determined by the Coomassie Blue binding assay (28) using bovine serum albumin as standard, and assuming a molecular mass of 216,000 daltons for PDE and 40,000 daltons for G α_t . The PDE concentration determined this way was 1.17-fold higher than that determined using the correction factor of Gillespie and Beavo (29) derived from amino acid analysis, and was 1.16-fold lower than that determined from UV absorbance, using a calculated $\epsilon_{280\text{ nm}}$ of 211,510 M $^{-1}$ cm $^{-1}$. When G α_t -GTP γ S concentrations determined by this assay were compared with those determined by radioactivity of purified protein prepared using GTP- γ - 35 S, the ratio was found to be 1.04.

Preparation of Vesicles—Lipids were mixed in organic solvent and dried down under a stream of N $_2$. For large unilamellar vesicle (LUV) preparations, the dried lipids were resuspended in aqueous buffer and subjected to at least 5 freeze/thaw cycles in liquid N $_2$. Lipid suspensions were then extruded 10 times through 0.1- μ m polycarbonate filters using either the Extruder (Lipex Biomembranes Inc.) or a Millipore stainless steel filter holder connected to an high performance liquid chromatography pump (12). Electron microscopy of dilute vesicle suspensions (Fig. 2D) confirmed that the extruded vesicles were predominantly unilamellar. For sucrose-loaded LUVs (sl-LUVs), 170 mM sucrose was included in the aqueous resuspension buffer prior to extrusion (30). After extrusion, the extravesicular [sucrose] was reduced to less than 1 mM by repeated dilution and pelleting in a TLA-100.3 rotor operating at 44,000 rpm. For small unilamellar vesicle (SUV) preparations, dried lipids were resuspended in aqueous buffer and sonicated for 10 cycles of 30 s at 4 °C in an ice bath. SUVs (20–40 nm diameter) were isolated by gel-filtration on a Sepharose CL-4B column (Ref. 31 and references cited therein).

Membrane Binding Assays (G $_t$)—G $_t$ was loaded with [α - 32 P]GTP by mixing with a catalytic amount of urea-washed ROS (G $_t$:R* molar ratio = 10:1). After GTP hydrolysis and the re-association of G $_t$ with G $\beta\gamma$, the membranes were pelleted and the G $_t$ -[32 P]GDP containing supernatant was collected and concentrated. For the vesicle-binding assay, G $_t$ -[32 P]GDP (100 nM) was mixed with sl-LUVs for 10 min at room temperature and pelleted in a TLA-100.3 rotor (Beckman) operating at 20 °C and 44,000 rpm. Total counts were measured in both the supernatant and the pellet. In some experiments, rhodamine-dipalmitoylphosphatidylethanolamine (Molecular Probes) was included at 0.1 mol % of the total lipid (with the remainder made up of PC with or without PS or cationic lipids) in the sl-LUVs, and vesicle pelleting efficiency was found, by fluorescence, to be greater than 95%.

Membrane Binding Assays (PDE)—When PDE was incubated with sl-LUVs, the pelleting assay was similar to that used for G $_t$ except the assays were performed in PDE assay buffer, or Low salt 3 buffer supplemented as indicated with NaCl, and the amount of PDE pelleted was determined by measuring trypsin-generated PDE activity. For PDE binding to other vesicle types, PDE-membrane complexes were pelleted in an airfuge operating at 28 p.s.i. at room temperature (12).

PDE Activity Assay—PDE activity was monitored by the pH assay (32) which detects the accumulation of protons following cGMP hydrolysis. Assays were conducted in pH assay buffer or Low salt 3 buffer supplemented with NaCl (50 mM unless indicated otherwise) and an initial cGMP concentration of 2 mM. Assays were carried out in 96-well microtiter plates maintained at 23 °C and monitored with either MI-410 or MI-415 microelectrodes (Microelectrodes Inc.) as described previously (12). At the conclusion of each assay, maximal PDE activation was determined through trypsin digestion of the inhibitory PDE γ subunit.

Curve Fitting—All of the plotted G $_t$ membrane binding data have been fit to the Hill equation with the program PSI-Plot (version 5.02c for Windows) which implements the Marquardt-Levenberg algorithm for multiparameter least-squares fitting. For each fit, in the equation,

$$G_{t,\text{bound}} = G_{t,\text{max}} \times [L]^n / (K^n + [L]^n) \quad (\text{Eq. 1})$$

² T. G. Wensel and Z. Yang, unpublished observations.

was solved for the Hill coefficient (n), with $K' = ([L] \text{ at } 0.5 \times G_{t,\text{max}})^n = ([L]_{0.5})^n$, where $[L]$ refers to total accessible lipid concentration in experiments where lipid was varied, and to G_t concentration in experiments where G_t was varied. "Accessible lipid" represents half of the total lipid, an approximation of the amount of lipid in the outer, exposed leaflet of the bilayer of LUVs, based on the determination here and in previous work (12) of their size distribution and predominantly unilamellar character. For SUVs, the difference between the areas of the interior and exterior leaflets was taken into account. $G_{t,\text{max}}$ = maximum G_t bound, expressed as percent of total where total G_t was constant, and in terms of concentration, when G_t was varied. The best fits, as determined by standard least squares criteria, are plotted as continuous curves.

Data for G_{α_t} -GTP γ S-PDE activation by liposomes were fit to the hyperbolic binding curve,

$$\text{PDE} = (\text{PDE}_{\text{max}} \times [\text{lipid}]) / (nK_d + [\text{lipid}]) \quad (\text{Eq. 2})$$

where PDE = % PDE activity at a particular concentration of accessible lipid ($[\text{lipid}]$), PDE_{max} = maximal PDE activity, and nK_d = (dissociation constant \times number of lipids involved in the binding site). Titrations of liposome-bound PDE with G_{α_t} -GTP γ S were analyzed as described (12, 33) for the "tight binding" case where the apparent dissociation constant is comparable to or much less than the concentrations of both proteins.

Formation of Ordered Planar Arrays of G_t —Ordered arrays of G_t were grown using the lipid-layer technique for two-dimensional crystallography (34). Briefly, various lipid mixtures (0–100% DSTAP or DOTAP or 0–40% stearylamine, with dioleoyl-PS, dioleoyl-PE, egg PE, DOPC, egg PC, or diphytanoyl-PC as filler) in 1:1 chloroform:hexane were floated over G_t (0.2 mg/ml) in Teflon wells. Buffer composition and crystallization conditions were varied to test a range of pH 5–11, ionic strength (0–50 mM NaCl), buffer (MOPS and Tris), temperature (0, 4, and 20 °C), and time (30 min to several days). Samples were screened by electron microscopy and ordered arrays were discovered only on 20:80 (mol/mol) DSTAP:diphytanoyl-PC or 20:80 (mol/mol) DOTAP:diphytanoyl-PC monolayers in Low salt 2 buffer. Arrays formed in 1–2 h at 4 °C.

Electron Microscopy—For cryo-EM of vesicle preparations, samples were applied to electron microscope grids covered with a holey-carbon film (35). Excess solution was wicked off and the grid was rapidly plunged into liquid ethane. Samples were then kept at or below liquid N_2 temperatures. The vesicles were imaged in a JEOL 1200 EX operating at 100 kV on a Gatan cryo-stage maintained at < -162 °C (36). Images were taken at a magnification of $\times 30,000$ and digitized on a Zeiss (model SCAI) microdensitometer with a 14- μm step size. For negatively stained planar arrays, monolayers were transferred from the air-water interface to carbon-coated continuous nitrocellulose electron microscope grids, washed with 1% uranyl acetate and imaged in a JEOL 100 CX operating at 80 kV. Images were taken at $\times 33,000$ magnification and digitized with a 7- μm step size.

RESULTS

Weak and Heterogeneous G_t Binding to Neutral and Negatively Charged Vesicles—When G_t was incubated with neutral PC vesicles at moderate ionic strength (Fig. 1), the accessible lipid concentration required for half-maximal binding ($[L]_{0.5}$) was about 170 μM , and was fairly insensitive to a reduction in ionic strength; the $[L]_{0.5}$ value increased only to 400 μM . Surprisingly, given the net negative electrostatic charge on G_t , binding to anionic PS-containing vesicles was about 3-fold stronger, with an $[L]_{0.5}$ value of 53 μM . The presence of the divalent cation Mg^{2+} in all of our buffers may be responsible for enhancing interactions between these two anionic species (37). Lowering the ionic strength reduced the affinity for negatively charged vesicles about 2-fold to an $[L]_{0.5}$ value of 110 μM .

An interesting feature of G_t binding to both neutral and anionic vesicles is that the maximum amount bound amounts to only about half of the total G_t added, and increasing the vesicle concentration up to 2 mM accessible lipid does not induce binding of the remaining G_t . The simplest explanation for this result is that the purified G_t , while homogeneous in its chromatographic and electrophoretic behavior, is heterogeneous with regard to its ability to bind these membranes. To test

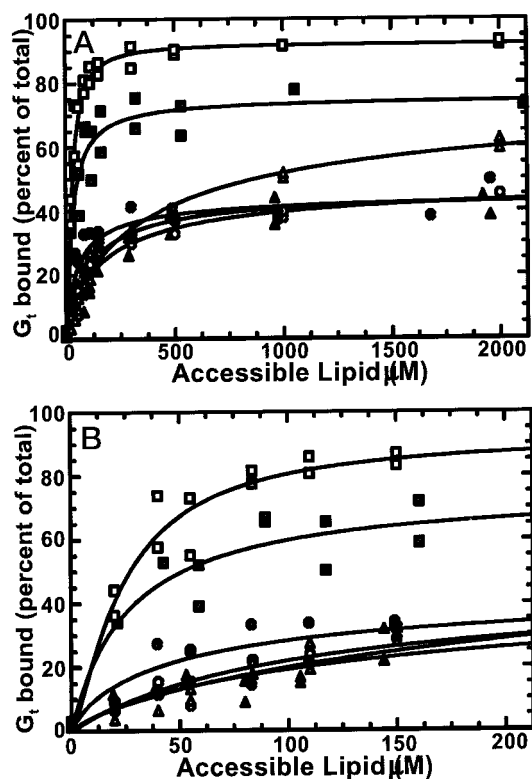


FIG. 1. Effects of ionic strength and lipid head group on G_t binding. G_t (100 nM) was mixed with sl-LUVs of differing compositions and binding was determined in either Low salt 2 buffer (open symbols) or in ROS buffer (filled symbols). Vesicle compositions are neutral (egg PC; triangles), anionic (20:80, mol/mol PS:egg PC; circles), and cationic (20:80, mol/mol, DSTAP:egg PC; squares). Fits are to the Hill equation with calculated $[L]_{0.5}$ values (expressed in terms of accessible lipid) and Hill coefficients (in parentheses) of: open squares, 24 μM (1.3); filled squares, 26 μM (1.0); open circles, 110 μM (1.0); filled circles, 53 μM (0.8); open triangles, 400 μM (0.8); filled triangles, 170 μM (0.8). A shows the full data set, while B shows the lower concentration points on a 10-fold expanded concentration scale.

whether the unbound G_t in these experiments was competent to bind vesicles, we incubated the unbound G_t in a supernatant from a PC sl-LUV binding assay with a fresh aliquot of PC vesicles in moderate salt (ROS) buffer. Less than 10% ($8.6\% \pm 2.6\%$) of this protein bound the vesicles when incubated at a lipid:protein ratio of 1.4×10^4 (1.4 mM accessible lipid).

Enhancement of Binding and Reduction of Heterogeneity by Positively Charged Lipids—Incorporation of positive charges into membranes lead to the highest affinity interactions, so that in moderate salt, $[L]_{0.5}$ is about 26 μM with PC vesicles containing 20 mol % DSTAP. Lowering ionic strength has little effect. The most striking difference between the positively charged vesicles and the others is that they seem to allow nearly all (>89%) of the added G_t to bind at concentrations of less than 500 μM accessible lipid.

G_t Aggregation of Cationic Vesicles—A feature of G_t binding to cationic vesicles that is not immediately obvious from the plot in Fig. 1 is its apparent cooperativity (see values of Hill coefficients in Fig. 1, legend). This cooperativity is more clearly seen at low lipid concentrations as shown in Fig. 2, A and B, where the Hill coefficients calculated varied from 1.3 to 4.3. This cooperativity was observed in both low and moderate salt, and with various kinds of positively charged lipids. The least pronounced cooperativity ($n = 1.3$) was observed with DSTAP; however, this apparently lower Hill coefficient may simply reflect the fact that this lipid mixture displays the highest affinity binding, obscuring cooperativity in the concentration range tested.

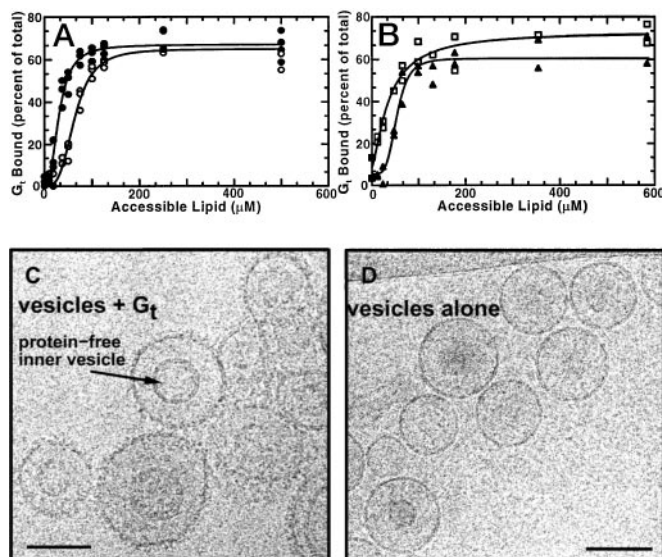


FIG. 2. Sigmoidal binding behavior and vesicle aggregation promoted by cationic vesicles and G_t . Vesicle pelleting binding assays were carried out on 100 nM G_t in the presence of increasing [cationic vesicles] in Low salt 2 buffer. *A*, binding assays on vesicles composed of either 20% stearylamine (open circles) or 40% stearylamine (filled circles) and egg PC. Solid lines are best fits of the Hill equation with $n = 3.3$ (open circles) and 2.5 (filled circles), respectively. *B*, binding assays to 20:80, mol/mol, DSTAP:DOPC (squares) and DOTAP:diphytanoyl-PC (triangles), in ROS buffer. Solid lines are best fits of the Hill equation with $n = 1.4$ (squares) and $n = 4.3$ (triangles). *C* and *D*, aggregation of cationic vesicles by G_t . DOTAP:diphytanoyl sLUVs (20:80, mol/mol, 200 μ M total lipid) were allowed to incubate with G_t (1 μ M, *C*) or without G_t (*D*) for 10 min on ice in Low salt 2 buffer. Samples were imaged at $\times 30,000$ magnification in a JEOL 1200 cryo-EM operating at 100 kV. Scale bars = 100 nm.

Cooperativity of this sort requires contributions to binding by more than one vesicle simultaneously, and a simple explanation for this sort of behavior could be cross-linking of vesicles. Electron microscopy of the G_t -vesicle complexes (Fig. 2, *C* and *D*) revealed that G_t is indeed able to bridge cationic vesicles. When DOTAP:diphytanoyl-PC vesicles were prepared in the absence of protein (Fig. 2*D*), individual spherical vesicles were observed. However, when these vesicles were incubated with G_t , they formed large aggregates and many of the vesicles were greatly deformed, presumably due to the "sandwiching" effect of a large layer of protein attracting two membrane surfaces together (38). The high density of protein packed onto the outer membrane surface gives rise to the rough appearance of the vesicle outer surfaces. Vesicles trapped within other vesicles are protein-free and appear smooth. Individual protein densities are surprisingly easy to see in the images. These densities jut out from the membrane ~ 75 Å, which would suggest that G_t is oriented with its longest axis almost perpendicular to the membrane surface.

Effects of Neutral and Anionic Membrane Surfaces on G_t -GTP γ S Stimulated PDE Activity—To determine the effects of lipid composition on G_t stimulation of PDE activity, we incubated PDE with various vesicle types and followed cGMP hydrolysis after addition of a 50-fold excess of G_t -GTP γ S (Fig. 3). The highest levels of activity were seen on LUVs composed of the unsaturated phospholipid DOPC, on which G_t -GTP γ S-stimulated PDE activity approached 75% of that observed following activation by trypsin. On either neutral or anionic LUVs with saturated phospholipids, PDE was only about 57% as active. Of all the synthetic membranes, those most highly curved (SUVs) were the least effective sites for PDE activation. Although insertion of the lipid tails on PDE and on G_t is likely required for efficient activation, the enhanced accessibility of

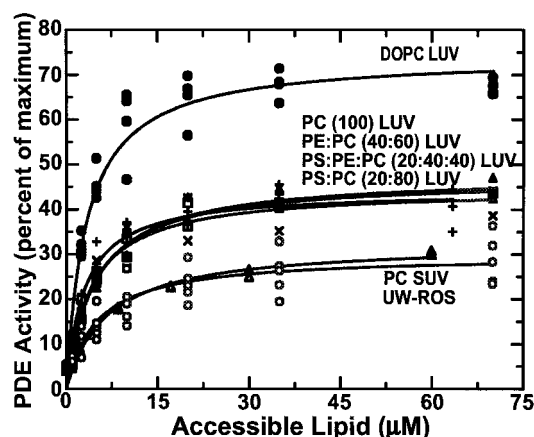


FIG. 3. Lipid dependence of PDE activation on liposomes. G_t -GTP γ S stimulated PDE activity was measured on various liposomes. 10 nM PDE was incubated with increasing concentrations of vesicles in PDE assay buffer with 150 mM KCl, and then activated by the addition of 0.5 μ M G_t -GTP γ S. Activity was monitored by the pH assay and the assay was initiated by the addition of 2 mM cGMP. Activity is plotted as percent of trypsin-generated activity. Smooth lines indicate best fits to Equation 2. Vesicle compositions and calculated K_d values (μ M, in parentheses) for each sample are: filled circles, DOPC LUVs (6.7); filled triangles, PE:PC, 40:60 mol/mol, LUVs (9.6); open squares, PS:PE:PC, 20:40:40, mol/mol/m, LUVs (9.9); \times , PS:PC, 20:80, mol/mol, LUVs (8.1); plus signs (+), PC LUVs (6.1); open triangles, urea-washed ROS (13.2); and open circles, PC SUVs (10).

the hydrocarbon phase offered by highly curved surfaces appears less important than the availability of a flat surface. As observed previously (12), ROS membranes were less efficient than PC LUVs at supporting PDE activation, and in fact were less efficient than any of the LUVs tested, consistent with the hypothesis that it is the lipid surface and not the major integral membrane protein rhodopsin that accounts for stimulation of G_t -PDE interactions by native membranes.

Potent Activation of PDE on Cationic Membranes—In contrast to PDE activation on neutral or charged surfaces, which requires a large excess of G_t -GTP γ S to activate nanomolar PDE, activation on positively charged vesicles (Fig. 4) occurred at near stoichiometric ratios of G_t -GTP γ S to PDE inhibitory or catalytic subunits. At a G_t -PDE ratio of 2:1 with liposomes containing the positively charged lipids DOTAP or DSTAP (Fig. 4), PDE activity was stimulated to levels ranging from 55% to greater than 80% of the level induced by trypsinization at PDE concentrations on the order of 10 nM. Under the same conditions neutral phospholipids allow for essentially no PDE activation. Little increase was seen in this activation when PDE was incubated for 3 h with the positively charged vesicles, suggesting that slow processes of protein reorganization or disaggregation did not play a major role.

The activation required G_t -GTP γ S at the salt concentration used of 50 mM NaCl (in PDE assay buffer, Fig. 4). Very little PDE activity was observed when no G_t -GTP γ S was added, or when $G\beta\gamma$ -GDP was added instead (Fig. 4). Consistent with the well known activation of PDE by polycations in the absence of G protein (39), cationic vesicles in low salt activate PDE without addition of G_t (Fig. 5); however, this mode of activation is negligible in the presence of 50 mM NaCl, while nearly 100% of PDE is bound to the vesicles at the same salt concentration.

Stoichiometry of PDE Activation by Transducin—Given that each PDE contains two subunits (α and β) containing conserved catalytic domains, and also contains two inhibitory subunits, it might be expected that there are two catalytic sites and two sites for binding by G_t . The enhancement of PDE- G_t interactions by cationic vesicles allowed us to investigate the correlation between PDE activation and binding of G_t . As shown in

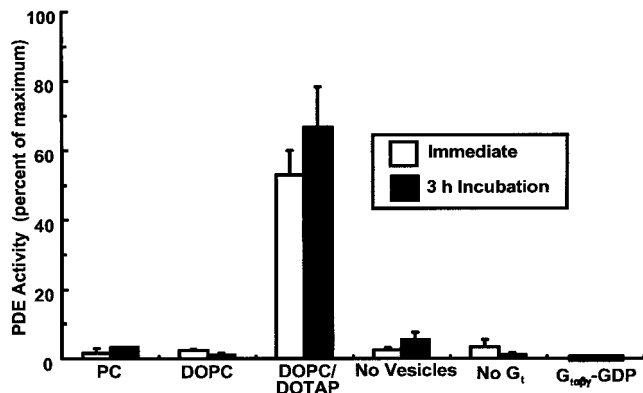


FIG. 4. Efficient PDE activation by G_{α_t} -GTP γ S on DOTAP. G_{α_t} -GTP γ S dependent activation of PDE was measured on a variety of vesicle surfaces in PDE assay buffer with 50 mM NaCl. PDE (10 nM) was added to vesicles (125 mM total lipid; egg PC, DOPC or 20:80 mol/mol DOTAP:DOPC), mixed, and then G_{α_t} -GTP γ S (20 nM) was added. For comparison, $G_{\alpha\beta\gamma_t}$ -dependent activation of PDE was measured on DOTAP:DOPC vesicles. Assays were initiated by the addition of 2 mM cGMP either immediately (open bars) or after a 3-h incubation (filled bars). G_{α_t} -GTP γ S dependent activity is plotted as percent of final trypsin generated activity. For each condition, $n = 2$.

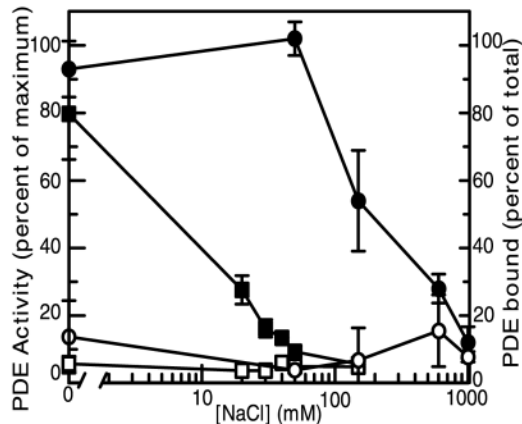


FIG. 5. Salt dependence of PDE binding and activation on DOTAP vesicles. The effects of increasing [NaCl] on DOTAP-dependent PDE activation and on maximal PDE binding were measured on 80:20, DOPC:DOPC sl-LUVs liposomes. Binding (circles), 15 nM PDE was mixed with sl-LUVs (filled circles, 25 mM total lipid) and without sl-LUVs (open circles), and % bound was determined by following trypsin activation of PDE in the supernatants and pellets. Activation (squares), 10 nM PDE was mixed with sl-LUVs (filled squares, 200 μ M total lipid), and without sl-LUVs (open squares) in Low salt 3 buffer, and PDE activity monitored. Activities are plotted as percent of the maximal trypsin generated activity. All points represent duplicate measurements.

the inset to Fig. 6, a salt and vesicle concentration can be chosen at which G_{α_t} binds only weakly to vesicles until PDE is added. PDE binds tightly to the vesicles in the absence of G_{α_t} under these conditions, but it enhances membrane binding of G_{α_t} , as observed previously for neutral vesicles (12). Thus, the increase in G_{α_t} bound to vesicles can be attributed to binding of G_{α_t} -GTP γ S to membrane-bound PDE, and it can be inferred that the great majority, if not all, of the vesicle bound G_{α_t} -GTP γ S is bound to PDE. Comparison of the molar ratios of bound G_{α_t} -GTP γ S/PDE, to PDE activation levels measured at various concentrations of added G_{α_t} -GTP γ S (Fig. 6) leads to a surprising conclusion: PDE is half-maximally activated when there is only one bound G_{α_t} for every two PDEs, or one G_{α_t} bound for every four PDE γ subunits, and PDE is maximally activated when there is slightly more than one G_{α_t} -GTP γ S bound to the vesicles per PDE. The most straightforward explanation of this result is that binding of one G_{α_t} -GTP γ S fully

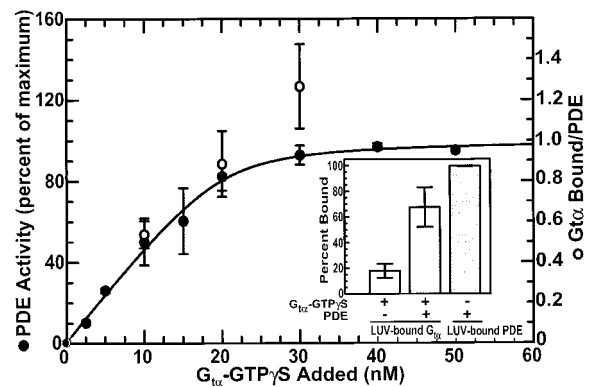


FIG. 6. Correlation of G_{α_t} -GTP γ S binding and PDE activation on DOTAP vesicles (20:80, DOTAP:DOPC sl-LUVs, 150 μ M accessible lipid). Inset, G_{α_t} -GTP γ S-independent binding of PDE, and PDE-dependent binding of G_{α_t} -GTP γ S. The percent of each protein bound was determined by densitometry of Coomassie Blue-stained bands following SDS-polyacrylamide gel electrophoresis of supernatant and pellet fractions from sedimentation. Less than 5% of either PDE or G_{α_t} -GTP γ S was in the pellet fraction when no vesicles were included. Where indicated, PDE was present at 9.7 nM, and G_{α_t} -GTP γ S was present at 20 nM. PDE activity (\bullet) and G_{α_t} -GTP γ S binding (\circ) as a function of G_{α_t} -GTP γ S added to PDE (9.7 nM) bound to cationic vesicles (20:80, DOTAP:DOPC sl-LUVs), 75 μ M accessible lipid). PDE activity results were fit to the equation $p = P_b + (P_{max} - P_b) [(K + P_{tot} + fG) - ((K + P_{tot} + fG)^2 - 4P_{tot}fG)^{-1/2}] / 2P_{tot}$, where P_b was the measured basal activity (6.44% of the maximal), G is the added G_{α_t} -GTP γ S, and the other parameters (K , f , P_{max}) were derived from the fit. For the data shown, K was 0.55 nM, f was 42%, and P_{max} was 70% of the trypsin-activated level. Both the data (\bullet) and the best fit curve are plotted as $100\% \times (P - P_b) / (P_{max} - P_b)$. Results are mean \pm S.D., of triplicate samples. The results in the main panel and the inset were obtained with separate preparations of PDE and G_{α_t} -GTP γ S.

activates PDE, and that either there is only one catalytic site, or there are two that are simultaneously activated by a single G_{α_t} -GTP γ S.

Effects of Proteolytic Removal of Lipid Modifications on PDE Activation—The amino terminus of G_{α_t} , and the carboxyl termini of PDE α and $-\beta$, have covalently attached lipids, and can be removed by well characterized limited proteolytic digestion procedures (27, 40). When the NH_2 -terminal fatty acyl moiety of G_{α_t} was removed along with the first 18 amino acids, PDE activation was almost completely eliminated (Fig. 7). In contrast, when the isoprenylated COOH termini of the PDE α and β subunits were removed, and the inhibitory PDE γ subunit added back, G_{α_t} -GTP γ S-stimulated PDE activity was comparable to that of native PDE. Thus efficient formation of the active PDE- G_{α_t} -GTP γ S complex on the cationic membrane surface requires the NH_2 -terminal lipidated peptide of G_{α_t} , but not the COOH-terminal peptides and lipids of PDE.

Two-dimensional Crystallization on Cationic Lipids—Electron crystallography (see review in Ref. 41) represents a potentially powerful approach for determining the structures of membrane-bound protein complexes, such as those involved in phototransduction. Formation of two-dimensional crystals suitable for structural studies has been accomplished for a number of soluble or peripheral membrane proteins. In general, these have required high affinity interactions between the proteins and the lipid (usually monolayer) surface. The relatively low affinity of G_t and the G_{α_t} -GTP γ S-PDE complex for neutral and anionic lipids poses a considerable challenge for two-dimensional crystal formation. We explored the possibility that the added attractive forces obtained by incorporation of positively charged lipids might allow us to pack these proteins onto membranes at high enough densities to allow ordered arrays to form. Fig. 8 shows that G_t displays an effective K_d for cationic vesicles of $\sim 1 \mu$ M and using very mild conditions can easily be

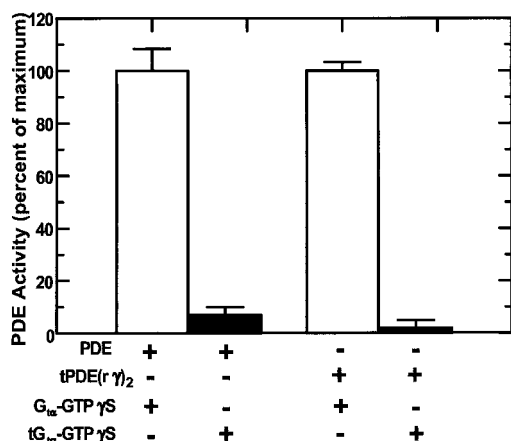


FIG. 7. Loss of PDE activation upon removal of G α_t lipid-modified NH₂ terminus. PDE (13.5 nM) activity was measured on 20:80, DOTAP:DOPC sl-LUVs in the presence of 20 nM G α_t -GTP γ S. tPDE(r γ)₂ indicates protein that had been subjected to partial proteolysis resulting in the loss of membrane binding lipid termini and the γ subunit, which was then replaced with recombinant γ . G α_t refers to intact G α_t -GTP γ S (*open bars*), and tG α_t -GTP γ S to partially proteolyzed G α_t -GTP γ S (*filled bars*), lacking its fatty acylated NH₂ terminus. Activities are plotted as values normalized to results with intact G α_t -GTP γ S.

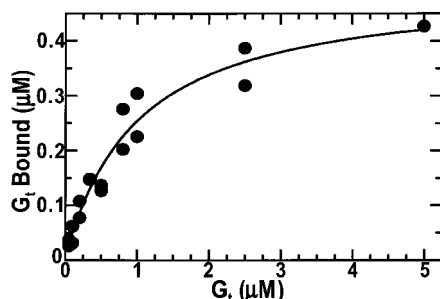


FIG. 8. G_t binding capacity of cationic membranes. Vesicle binding assays were carried out with increasing [G_t] in the presence of 20:80, DSTAP:egg PC sl-LUVs (48.5 μ M total lipid) in Low salt 2 buffer. The *solid line* is a best fit to the Hill equation with $n = 1.0$, $[L]_{0.5} = 1.0$ μ M, and $G_{t,max} = 0.43$ μ M, corresponding to maximal binding of one G_t per 110 surface lipids.

loaded onto membranes at densities up to 1 G_t per 113 lipids. This density approaches estimates for the G_t:lipid ratio expected for membranes saturated with randomly distributed G_t.

Using conditions similar to those that gave optimal G_t binding to vesicles, we spread monolayers of cation-containing lipid mixtures at the air-water interface, with G_t in the aqueous subphase. After screening multiple variations of lipid composition and protein concentration, we found that small ordered arrays formed on monolayers containing either 20% DSTAP or DOTAP with 80% diphytanoyl-PC (Fig. 9, *left*). Computed diffraction patterns (Fig. 9, *left, inset*) obtained by calculating the Fourier transforms of these images of these arrays revealed well resolved peaks indicating a local crystalline lattice. Fourier filtering the images (Fig. 9, *right*) revealed the pattern of protein density more clearly, allowing the identification of individual G_t molecules. In Fig. 9, *right*, we have superimposed the ribbon diagram of the G_t x-ray structure (42) in three orthogonal orientations to illustrate that each density is approximately the size of a single G_t. At higher resolution it should be possible to distinguish which orientation G_t assumes on the membrane surface. Preliminary results suggest that more highly ordered G_t arrays can be formed under some conditions (43), and that G α_t -GTP γ S-PDE complexes can also be packed onto cationic lipid surfaces at densities appropriate for two-dimensional crystallization.

DISCUSSION

Lipid Properties and Formation of Signaling Complexes—To evaluate the contributions of lipid structure to membrane-dependent signaling complex formation, we have reconstituted protein complexes on synthetic liposomes. To test for electrostatic contributions, charged lipids were included at 20 mol % of the total lipid, which is similar to the lipid charge density in ROS disc membranes where the anionic lipid population is ~15% of the total lipid (44, 45) and has an asymmetric distribution which concentrates the charge on the cytoplasmic face (46). We have found that in the absence of these charged lipids, G_t binds membranes less tightly. The surprising observation that binding is enhanced on liposomes containing *either* anionic or cationic lipids is consistent with a model in which an anionic patch on G_t associates directly with cationic lipids or indirectly, through a Mg²⁺ bridge, with anionic lipids, as has been suggested previously (37). Positive charges also allowed a much greater fraction of the protein to bind, suggesting that a major effect of the positive charges is to promote formation of protein-membrane complexes that induce conformational changes allowing membrane insertion of the lipid moieties attached to the proteins. This effect is most striking with respect to G_t and G α_t -GTP γ S, whose functional heterogeneity is largely eliminated by the positively charged membranes. This mode of activation may be similar to the induced “surface activation” of transducin by divalent cations, which was shown to involve increasing the hydrophobic interactions of the protein with the membrane (37). The positive charges may also act on surface pressure, a parameter important for membrane affinity (37). Because it would be hard to explain the physiological responses of rod cells to light if G_t-PDE interactions were as inefficient as typically observed in reconstituted systems with negatively charged or neutral lipids, it seems likely that the interactions on the positively charged membranes more closely resemble those present in intact cells with the native proteins.

The enhancing effects of side chain unsaturation (DOPC) and methylation (diphytanoyl-PC) on G_t and PDE interactions with membranes are consistent with the overall composition of disc membranes. About half of the fatty acids of disc membranes are unsaturated, and ~30% of the side chains are the bulky and highly unsaturated docosahexaenoyl (C22:6) (44). A poorly understood but highly effective recycling system maintains C22:6 at high levels in ROS membranes even when it is depleted from other tissues. One functional role for C22:6 may be to facilitate insertion of the lipid moieties on G_t and PDE. The idea that the lipid groups only, and not significant portions of the peptide chains themselves, are inserted into the membrane is supported by the observation that the highly curved surface of SUVs does not support efficient formation of the PDE-G α_t -GTP γ S complex (*cf.* Ref. 47).

Functional Heterogeneity of G_t and G α_t -GTP γ S and the Effects of Cationic Lipids—A number of studies have reported evidence of functional heterogeneity of G_t as revealed by PDE activation and membrane binding (12, 14, 24, 48). The only chemical differences that have been found for functionally distinct pools of G_t are the different NH₂-terminal fatty acyl chains (3, 4, 6, 49) but these appear to give rise to only subtle differences in the ease of extraction of G_t from membranes (48). Thus differences in protein conformation, rather than covalent differences, seem most likely to account for the striking difference observed in PDE activation and in membrane binding, which are strongly correlated with one another (12, 14). In several cases of lipidated proteins with known three-dimensional structures (50–53), the lipid moieties are found not projecting away from the protein and exposed to solvent, as would be expected when they are inserted into the hydrocarbon

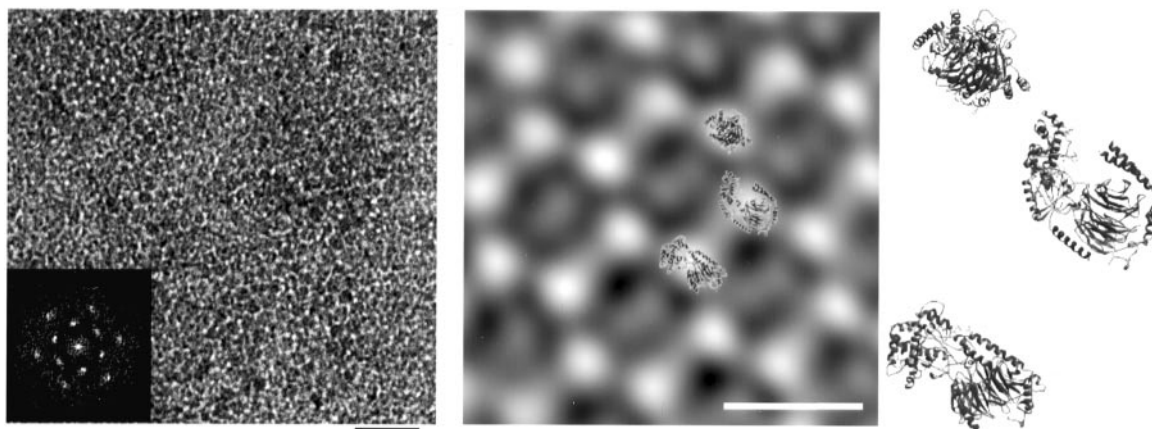


FIG. 9. **Small ordered arrays formed by G_t on cationic monolayers.** *Left*, two-dimensionally ordered arrays of G_t were grown on 20:80, mol/mol, DSTAP:egg PC monolayers. The monolayers were transferred to carbon-coated continuous nitrocellulose electron microscope grids and stained with 1% uranyl acetate. The image was taken at $\times 33,000$ magnification on a JEOL 100 CX operating at 80 kV. Scale bar = 100 nm. Shown in the *inset* is a computed Fourier transform with reflections out to ~ 80 Å. *Right*, the largest and most ordered arrays were Fourier-filtered to reduce noise and identify the repeating G_t densities. Scale bar = 16 nm. A ribbon diagram of the G_t x-ray structure is shown superimposed in three orthogonal orientations to demonstrate that the size is consistent with each density being an individual heterotrimer and to suggest the potential application of this approach to determine protein orientation on membrane surfaces.

phase of phospholipid membranes, but rather tucked into hydrophobic pockets either on the surface, or buried fairly deeply. There are two well documented cases of lipidated rod outer segment proteins, which undergo conformational changes involving lipid sequestration when removed from membranes. In the structure of $G\beta\gamma_t$ complexed to phosducin (53) the farnesyl group of $G\gamma_t$ is seen inserted into a pocket not seen in the structure of $G\beta\gamma_t$ alone (54) or bound to $G\alpha_t$ (42). In the structure of recoverin, a dramatic conformational change is seen when the non-lipidated calcium-bound form is compared with the calcium-free myristoylated form (52, 55). A structure has been determined for fatty acylated recoverin in the calcium-bound form, which does show the lipid projecting from the protein surface in a manner expected to facilitate membrane insertion (56). However, this form of the protein could only be maintained in monomeric soluble form by use of a fatty acid modified by hydroxylation to increase its hydrophilicity. Thus, a plausible explanation for G_t heterogeneity is that removal of G_t from disc membranes induces two or more conformational states that accommodate sequestration of the lipid groups, and only a subset of these states can readily convert to the native form with its high affinity for membranes and PDE. Based on the results presented here, we propose that cationic membranes facilitate conversion of the "intractable" conformations to this native-like state, much as calcium induces extrusion of the fatty acid from recoverin, thus facilitating its membrane attachment (57).

Models for G_t Activation of PDE—A number of models have been proposed for the mechanism of PDE activation, and for the subunit composition of the activated complex(es). The simplest suggestion, given that there are two PDE γ sites on holo-PDE, is that they are functionally equivalent, with roughly equal affinities for PDE γ binding to the catalytic subunits, and for $G\alpha_t$ binding to PDE γ on holo-PDE (17). Alternatively, it has been suggested that two classes of binding sites exist for PDE γ and/or $G\alpha_t$, with different affinities and/or contributions to catalysis or inhibition. These could arise from intrinsic differences between sites, or from binding at one site allosterically switching the properties of the other. Thus, apparent cooperativity for inhibition by PDE γ (20) and for $G\alpha_t$ activation of PDE (18) have been reported. We have failed to observe any hints of cooperativity in many titrations of PDE $\alpha\beta$ with PDE γ or of membrane-bound PDE $\alpha\beta\gamma\gamma$ with $G\alpha_t$ -GTP γ S in this or previous studies (12, 17, 33, 40). However, our current results

argue strongly in favor of a model in which, at least under the conditions employed here, the two sites for $G\alpha_t$ binding have dramatically different effects on activity, with the "first" one binding giving rise to full activation. This first binding event could either represent binding to a site with much higher intrinsic affinity for $G\alpha_t$ than the "second," or simply reflect the sort of allosteric switching referred to above. Recent results with modified forms of PDE γ (21) suggest that the former explanation is more likely.

Prospects for Structural Analysis of Transduction Complexes—Ultimately, determination of the nature of the activated $G\alpha_t$ -PDE complex will require analysis by direct structural methods. The membrane dependence of the interaction between $G\alpha_t$ -GTP γ S and PDE, and its weakness in solution, do not bode well for the formation of conventional three-dimensional crystals suitable for x-ray analysis. Likewise, it seems unlikely that the G_t -membrane complex structure will be solved by x-ray crystallography. Electron microscopy, however, is well suited for these problems, because individual molecules or monomolecular layers have sufficient electron scattering power for imaging, even in unstained ice-embedded samples (41). Reproducible formation of target complexes, and, ideally, sufficient packing densities to allow two-dimensional crystallization, are prerequisites for obtaining sufficient numbers of images to allow moderate-to-high resolution structures to be determined. The images presented in Figs. 2 and 9 have already provided some hints at how G_t binds membranes, and preliminary results indicate that more highly ordered structures with helical symmetry can be constructed using the same cationic lipid mixtures used here (43, 58).

REFERENCES

- Wensel, T. G. (1999) in *Introductory Signal Transduction* (Sitaramayya, A., ed) pp. 29–46, Birkhauser, Boston
- Anant, J. S., Ong, O. C., Xie, H. Y., Clarke, S., O'Brien, P. J., and Fung, B. K. (1992) *J. Biol. Chem.* **267**, 687–690
- Kokame, K., Fukada, Y., Yoshizawa, T., Takao, T., and Shimonishi, Y. (1992) *Nature* **359**, 749–752
- Neubert, T. A., Johnson, R. S., Hurley, J. B., and Walsh, K. A. (1992) *J. Biol. Chem.* **267**, 18274–18277
- Yang, Z., and Wensel, T. G. (1992) *J. Biol. Chem.* **267**, 23197–23201
- DeMar, J. C., Jr., Wensel, T. G., and Anderson, R. E. (1996) *J. Biol. Chem.* **271**, 5007–5016
- Fukada, Y., Takao, T., Ohguro, H., Yoshizawa, T., Akino, T., and Shimonishi, Y. (1990) *Nature* **346**, 658–660
- Lai, R. K., Perez-Sala, D., Canada, F. J., and Rando, R. R. (1990) *Proc. Natl. Acad. Sci. U. S. A.* **87**, 7673–7677
- Fung, B. K.-K., and Nash, C. R. (1983) *J. Biol. Chem.* **258**, 10503–10510
- Tyminski, P. N., and O'Brien, D. F. (1984) *Biochemistry* **23**, 3986–3993

11. Clerc, A., and Bennett, N. (1992) *J. Biol. Chem.* **267**, 6620–6627
12. Malinski, J. A., and Wensel, T. G. (1992) *Biochemistry* **31**, 9502–9512
13. Bruckert, F., Catty, P., Deterre, P., and Pfister, C. (1994) *Biochemistry* **33**, 12625–12634
14. Wensel, T. G., and Stryer, L. (1988) in *Enzyme Dynamics and Regulation* (Chock, P. B., Huang, C. Y., Tsou, C. L., and Wang, J. H., eds) pp. 102–112, Springer-Verlag, New York
15. Deterre, P., Bigay, J., Forquet, F., Robert, M., and Chabre, M. (1988) *Proc. Natl. Acad. Sci. U. S. A.* **85**, 2424–2428
16. Otto-Bruc, A., Antonny, B., Vuong, M., Chardin, P., and Chabre, M. (1993) *Biochemistry* **32**, 8636–8645
17. Wensel, T. G., and Stryer, L. (1990) *Biochemistry* **29**, 2155–2161
18. Bennett, N., and Clerc, A. (1989) *Biochemistry* **28**, 7418–7424
19. Clerc, A., Catty, P., and Bennett, N. (1992) *J. Biol. Chem.* **267**, 19948–19953
20. Whalen, M. M., and Bitensky, M. W. (1989) *Biochem. J.* **259**, 13–19
21. Berger, A. L., Cerione, R. A., and Erickson, J. W. (1999) *Biochemistry* **38**, 1293–1299
22. Papermaster, D. S., and Dryer, W. J. (1974) *Biochemistry* **13**, 2438–2444
23. Yamanaka, G., Eckstein, F., and Stryer, L. (1985) *Biochemistry* **24**, 8094–8101
24. Fung, B. K.-K., Hurley, J. B., and Stryer, L. (1981) *Proc. Natl. Acad. Sci. U. S. A.* **78**, 152–156
25. Ramdas, L., Disher, R. M., and Wensel, T. G. (1991) *Biochemistry* **30**, 11637–11645
26. Angleson, J. K., and Wensel, T. G. (1994) *J. Biol. Chem.* **269**, 16290–16296
27. Mazzoni, M. R., Malinski, J. A., and Hamm, H. E. (1991) *J. Biol. Chem.* **266**, 14072–14081
28. Bradford, M. M., (1970) *Anal. Biochem.* **72**, 248–254
29. Gillespie, P. G., and Beavo, J. A. (1989) *Proc. Natl. Acad. Sci. U. S. A.* **86**, 4311–4315
30. Rebecchi, M. J., Peterson, A. A., and McLaughlin, S. (1992) *Biochemistry* **31**, 12742–12747
31. Plager, D. A., and Nelsestuen, G. L. (1994) *Biochemistry* **33**, 7005–7013
32. Liebman, P. A., and Evanczuk, T. (1982) *Methods Enzymol.* **81**, 532–542
33. Malinski, J. A., Zera, E. Z., Angleson, J. K., and Wensel, T. G. (1996) *J. Biol. Chem.* **271**, 12919–12924
34. Uzgiris, E. E., and Kornberg, R. D. (1983) *Nature* **301**, 125–129
35. Fukami, A., and Adachi, K. (1965) *J. Electron Microsc.* **14**, 112–118
36. Avila-Sakar, A. J., and Chiu, W. (1996) *Biophys. J.* **70**, 57–68
37. Seitz, H. R., Heck, M., Hofmann, K. P., Alt, T., Pellaud, J., and Seelig, A. (1999) *Biochemistry* **38**, 7950–7960
38. Chiruvolu, S., Walker, S., Israelachvili, J., Schmitt, F. J., Leckband, D., and Zasadzinski, J. A. (1994) *Science* **264**, 1753–1756
39. Miki, N., Baraban, J., Keirns, J. J., Boyce, J. J., and Bitensky, M. W. (1975) *J. Biol. Chem.* **250**, 6320–6327
40. Wensel, T. G., and Stryer, L. (1986) *Proteins Struct. Funct. Genet.* **1**, 90–99
41. Chiu, W., McGough, A., Sherman, M. B., and Schmid, M. F. (1999) *Trends Cell Biol.* **9**, 154–159
42. Lambright, D. G., Sondek, J., Bohm, A., Skiba, N. P., Hamm, H. E., and Sigler, P. B. (1996) *Nature* **379**, 311–319
43. Melia, T. J., Sowa, M. E., Schutze, L., and Wensel, T. G. (1999) *J. Struct. Biol.* **128**, 119–130
44. Daemen, F. J. (1973) *Biochim. Biophys. Acta* **300**, 255–288
45. Miljanich, G. P., Nemes, P. P., White, D. L., and Dratz, E. A. (1981) *J. Membr. Biol.* **60**, 249–255
46. Tsui, F. C., Sundberg, S. A., and Hubbell, W. L. (1990) *Biophys. J.* **57**, 85–97
47. Silversmith, R. E., and Nelsestuen, G. L. (1986) *Biochemistry* **25**, 7717–7725
48. Neubert, T. A., and Hurley, J. B. (1998) *FEBS Lett.* **422**, 343–345
49. DeMar, J. C., Rundle, D. R., Wensel, T. G., and Anderson, R. E. (1999) *Prog. Lipid Res.* **38**, 49–90
50. Zheng, J., Knighton, D. R., Xuong, N. H., Taylor, S. S., Sowadski, J. M., and Ten Eyck, L. F. (1993) *Protein Sci.* **2**, 1559–1573
51. Griffith, J. P., Kim, J. L., Kim, E. E., Sintchak, M. D., Thomson, J. A., Fitzgibbon, M. J., Fleming, M. A., Caron, P. R., Hsiao, K., and Navia, M. A. (1995) *Cell* **82**, 507–522
52. Tanaka, T., Ames, J. B., Harvey, T. S., Stryer, L., and Ikura, M. (1995) *Nature* **376**, 444–447
53. Loew, A., Ho, Y. K., Blundell, T., and Bax, B. (1998) *Structure* **6**, 1007–1019
54. Sondek, J., Bohm, A., Lambright, D. G., Hamm, H. E., and Sigler, P. B. (1996) *Nature* **379**, 369–374
55. Flaherty, K. M., Zozulya, S., Stryer, L., and McKay, D. B. (1993) *Cell* **75**, 709–716
56. Ames, J. B., Ishima, R., Tanaka, T., Gordon, J. I., Stryer, L., and Ikura, M. (1997) *Nature* **389**, 198–202
57. Zozulya, S., and Stryer, L. (1992) *Proc. Natl. Acad. Sci. U. S. A.* **89**, 11569–11573
58. Melia, T. J. (1999) Ph.D. dissertation, Baylor College of Medicine, Houston, TX